Journal of
Nanoscience and Nanotechnology
Vol. 11, 4675–4683, 2011

Multifunctional Nanovehicles for Combined 5-Fluorouracil and Gold Nanoparticles Based on the Nanoprecipitation Method

Abeer Karmi[1], Ghaleb A. Husseini[1, 2, *], Maryam Faroun[1], and Mukhles Sowwan[1, *]

[1] *The Nanotechnology Research Laboratory, Materials Engineering Department, Al-Quds University, East Jerusalem*
[2] *Chemical Engineering Department, American University of Sharjah, Sharjah, United Arab Emirates*

To facilitate the administration of combined 5-Fluorouracil (5-FU) and gold nanoparticles (for photothermal treatment purposes), we developed 5-FU-gold-poly(lactide-co-glycolic acid) (5-FU-Au-PLGA) nanovehicles, via the nanoprecipitation method. The gold nanoparticles were incorporated inside the 5-FU-PLGA carriers using a roller mixer. Morphological analysis using atomic force microscopy (AFM), scanning electron microscopy (SEM) and transmission electron microscopy (TEM), indicated uniform, singly separated spherical nanoparticles (NPs). Drug content, recovery and entrapment in the NPs were approximated using UV-spectrophotometer data. Approximately 26% of nanoparticles were recovered after drying. The percentage of total drug content was about 30%, and the percentage of drug entrapment reached 57%. Electrostatic Force Microscopy images confirmed the presence of gold inside the drug-loaded nanoparticles. We speculate that the 20-nm gold particles were able to diffuse, after 12 hours of mixing (using the roller mixer), into the PLGA matrix through the 100-nm pores (observed by SEM) without affecting the integrity of the drug delivery vehicle. These synthesized nanoparticles show promise as multimodal vehicles in the delivery of chemotherapeutic agents.

Keywords: Drug Delivery, 5-Fluorouracil, PLGA, Nanoprecipitation Method, Gold Nanoparticles.

RESEARCH ARTICLE

1. INTRODUCTION

The past few years have witnessed an extraordinary growth and interest in the field of nanomedicine, whether in diagnosis or treatment of diseases. In particular, the design of drug delivery carriers that minimize the side effects of therapeutic agents has gained leviathan attention. These nanovehicles include liposomes,[1–3] polymeric micelles,[4–12] solid particles[13–20] and polymersomes.[21] Engineered nanoparticles intended for medical purposes have to be generally in the size range of 20–500 nm. These nanoparticles (NPs) have relatively large surfaces, which enhance their ability to bind, adsorb and carry other compounds such as drugs, probes and proteins. For drug delivery purposes, biodegradable nanoparticle formulations are preferred[22] with Poly (lactic-co-glycolic acid) (PLGA) nanoparticles being among the most studied solid biodegradable nanocarriers in drug delivery.

Several methods have been successful in nanoparticle preparation from biodegradable and biocompatible polymers including solvent evaporation, monopolymerization, nanoprecipitation, in addition to the salting out method.[23] Yang et al.[24] developed a system for diagnosing and treating breast cancer, based on doxorubicin (Dox)—magnetic PLGA nanoparticles conjugated with well-tailored antibodies. The goal of their study was to synthesize a multimodal nanocomposite drug delivery system composed of the anticancer drug Dox combined with the magnetic particles of ferrous-ferric oxide (Fe_3O_4) entrapped in PLGA nanoparticles using the nanoemulsion method. To achieve active targeting, the antibody Herceptin (HER) was conjugated on the surface of the nanocomposite.[24] In another study, nanoparticles for combined Dox and photothermal treatments were synthesized by Park et al.[25] The group developed Dox-loaded-PLGA-gold-half-shell nanoparticles (Dox-loaded PLGA-Au H-S NPs) by depositing gold films on Dox-loaded PLGA nanoparticles (PLGANPs) for Hela cells treatment. Dox is slowly released from the biodegradable PLGANPs.

*Authors to whom correspondence should be addressed.

Additionally, and in an attempt to improve the *in vivo* effectiveness of these nanocarriers, heat was locally generated by utilizing near-infrared (NIR) irradiation. In this paper, we report the incorporation of the hydrophilic antineoplastic agent 5-Fluorouracil (5-FU) and gold nanoparticles (GNPs) into PLGA carriers. We will also report on utilizing electrostatic force microscopy (EFM) as a novel characterization technique for nanoparticles.

2. METHODS AND MATERIALS

2.1. Materials

The polymer used in the production of the nanoparticles is poly(lactide-co-glycolic acid) (PLGA), (Sigma Aldrich, St. Louis, MO, USA), with a ratio of 75:25 lactide: glycolide, and a molecular weight range of 66,000–107,000. Dimethylformamide (DMF) (Sigma Aldrich, St. Louis, MO, USA) is used as the organic solvent, and triple distilled water as the aqueous phase. 5-Fluorouracil (5-FU) is obtained from the Pharmaceutical Research Laboratory (Al Quds University, Jerusalem).

2.2. Methods

2.2.1. Nanoparticles Preparation

The nanoprecipitation method used in this research is illustrated in Figure 1.[26] It is based on assembling an organic phase with an aqueous phase and forming a colloidal system. This method includes dissolving 82 mg of the PLGA copolymer and 50 mg of 5-FU in 2.7 ml DMF. Nanoprecipitation occurs when the organic phase comes in contact with 10 ml of the aqueous phase thus allowing for the formation of solid spherical homogenous nanoparticles. The organic phase is slowly added to the aqueous phase by inserting the syringe directly into the magnetically stirred dispersed phase and continuously stirring for 1 hour. The subsequent suspension is centrifuged 4 times for 15 minutes, and the resulting suspension is dried using a speed dryer at 35 °C for one hour. The nanoparticles are then washed three times with water in order to remove the traces of the 5-FU that adsorbed on their surface and to get rid of the excess DMF. Finally, the gold nanoparticles are incorporated inside the 5-FU/PLGA carriers using a roller mixer. Typically the 5-FU/PLGA and gold nanoparticles were allowed to mix for 12 hours.

2.2.2. Morphology

The morphological characterization of the empty, and the 5-FU loaded nanoparticles, is achieved using atomic force microscopy (AFM) (Nanotec Electronica, Madrid, Spain), scanning electron microscopy (SEM) (FEI Company, Hillsboro, Oregon, USA) and transmission electron microscope (TEM) (FEI Company, Hillsboro, Oregon, USA). The procedure involves placing a 20-μl drop on a mica substrate to study the morphology using AFM, a 10-μl drop on a silicon dioxide substrate to obtain SEM images, and a 5-μl drop on a copper grid for TEM characterization.

2.2.3. Dynamic Light Scattering (DLS)

Zetasizer Nanoparticle Analyzer (Malvern Instruments Ltd, Worcestershire, UK) is used to find the size of the nanocarriers. Each nanoparticle sample is diluted 10-fold for DLS analysis.

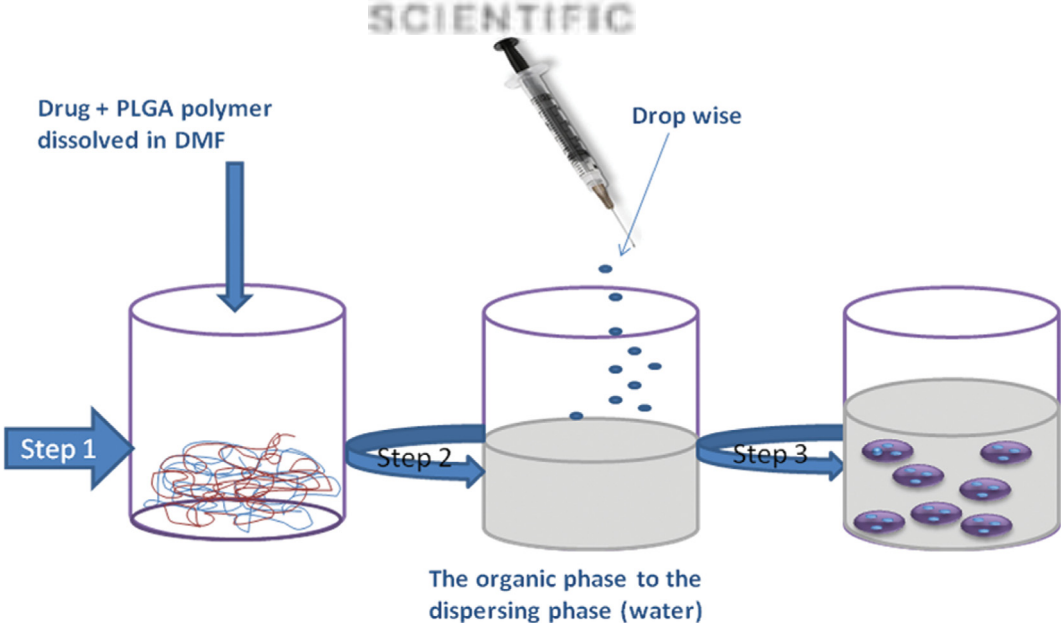

Fig. 1. Preparation of PLGA combined therapy nanosystems by nanoprecipitation method.

RESEARCH ARTICLE

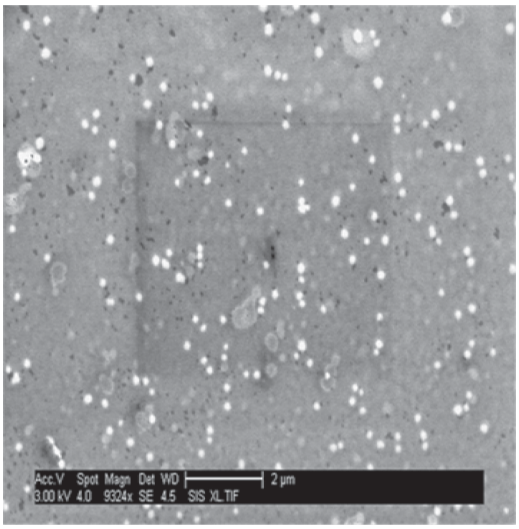

Fig. 2. SEM image of empty PLGA nanoparticles.

2.2.4. Determination of 5-FU Loading

The encapsulation efficiency of drug loading inside the nanoparticles is determined by measuring the amount of the non-encapsulated 5-FU in the supernatant (after centrifuging and washing the nanoparticles). The loading efficiency and the concentrations are measured and calculated using UV spectrophotometer data (NanoDrop Technologies, San Francisco, CA, USA). The following equation is used to calculate the percentage recovery of 5-FU in the collected nanoparticles.

$$\text{Nanoparticle Recovery (\%)} = \frac{\text{mass of nanoparticles recovered} \times 100\%}{\text{mass of polymeric material, drug and any exipient used in formulation}} \quad (1)$$

Equations 2 and 3 [23] are used to calculate the loading capacity and drug entrapment:

$$\text{Drug content (\% w/w)} = \frac{\text{mass of drug in nanoparticles} \times 100\%}{\text{mass of nanoparticles recovered}} \quad (2)$$

$$\text{Drug entrapment (\%)} = \frac{\text{mass of drug in nanoparticles} \times 100\%}{\text{mass of drug used in formulation}} \quad (3)$$

2.2.5. In-Vitro Release

In vitro release of 5-FU from the PLGA nanoparticles is studied using a spectrophotometer that measures the UV light absorbance of the drug at different time intervals. The drug loaded PLGA molecules are introduced into a continuously stirred (stirring being accomplished via a horizontal shaker) phosphate buffer saline (PBS) with a pH = 7.4 and a temperature of 37 °C. Aliquots are taken every two hours, and their absorbance measured at 265 nm (drug molecules absorb UV light at 265 nm but the empty PLGANP do not).

The cumulative amount of 5-FU released from drug-loaded PLGA nanoparticles is calculated using the following equation:

$$\text{Comulative Release (\%)} = \frac{M(t) \times 100\%}{M_{\text{actual}}} \quad (4)$$

Where, $M(t)$ is the mass of 5-FU released from the PLGANPs at time (t) and M_{actual} is the mass of 5-FU present in the PLGANPs, as calculated using Eq. (2).

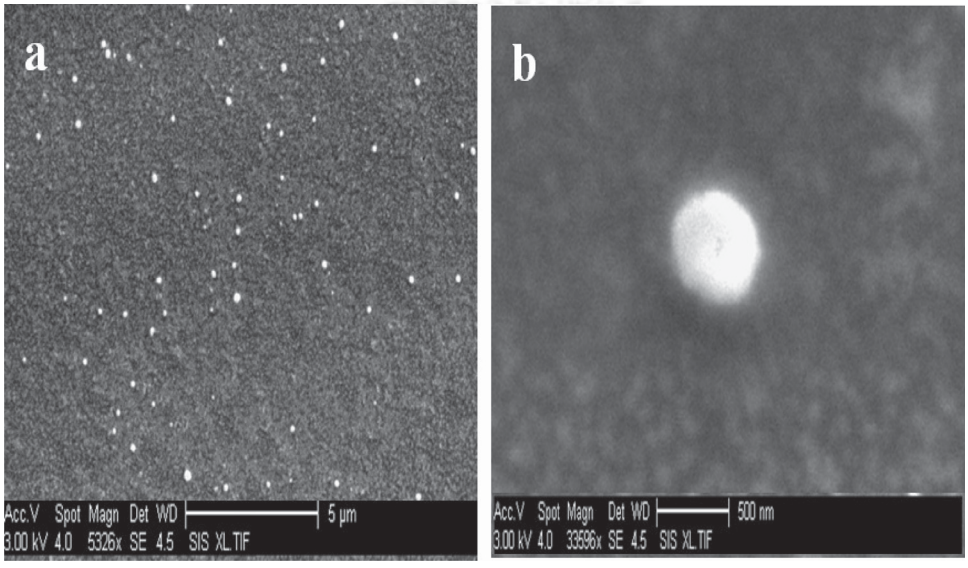

Fig. 3. SEM images. (a) Shows distribution of NPs loaded 5-FU, (b) zoom image for one NP drug loaded.

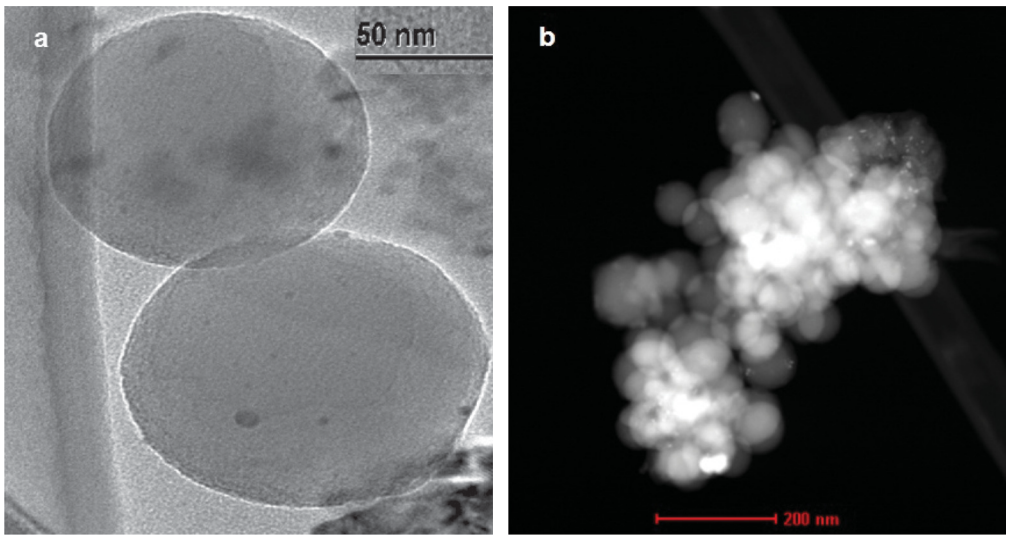

Fig. 4. TEM images of 5-FU loaded nanoparticles. (a) Zoom image, (b) shows distribution of loaded nanoparticles.

3. RESULTS AND DISCUSSION

3.1. Nanoparticle Morphology

A 10-μl drop of empty and drug-loaded nanoparticle samples is placed on a silicon dioxide substrate and then examined under a SEM. Figure 2 shows uniform singly-separated spherical nanoparticles with an average size of 192.02 nm.

Figure 3(a) shows the distribution of uniform spherical-singly separated 5-FU nanoparticles with an average size of 251.2 nm. By zooming to the nanoscale, Figure 3(b) confirms the spherical shape of these novel carriers.

In order to further characterize the physical shape of these nanoparticles, a 5-μl drop of 5-FU loaded nanoparticles is deposited on a copper grid for TEM characterization. Figure 4 shows the morphology of the

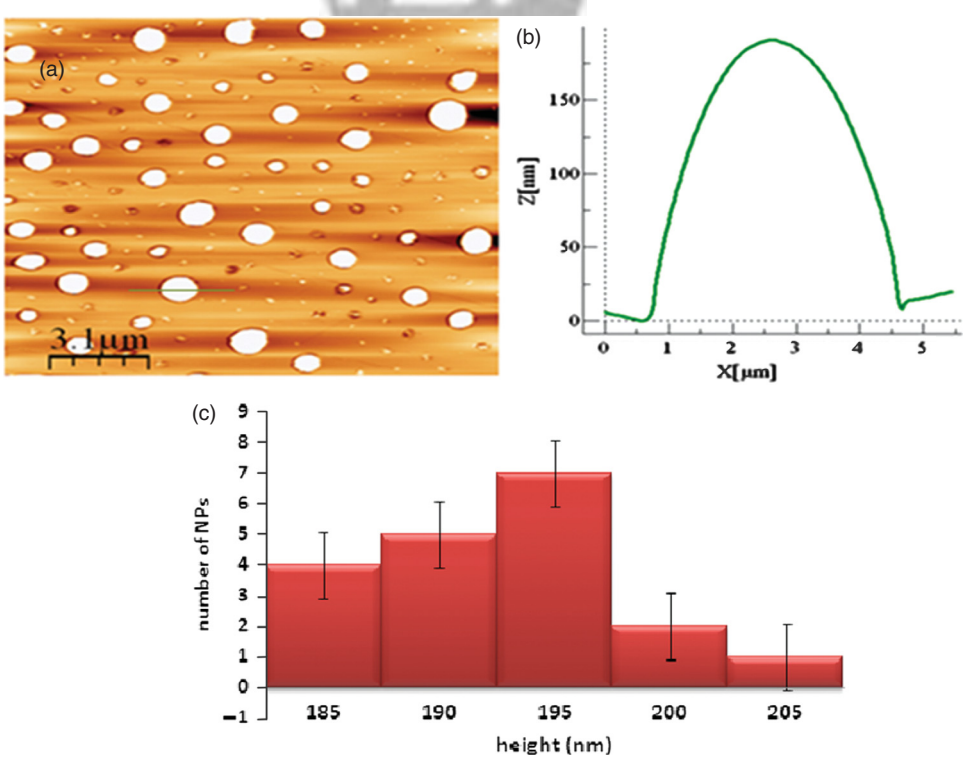

Fig. 5. AFM topography images for empty nanoparticles. (a) Shows singly separated NPs. (b) Cross sectional height profile of single NP. (c) Histogram shows the height distribution of empty PLGA NPs.

RESEARCH ARTICLE

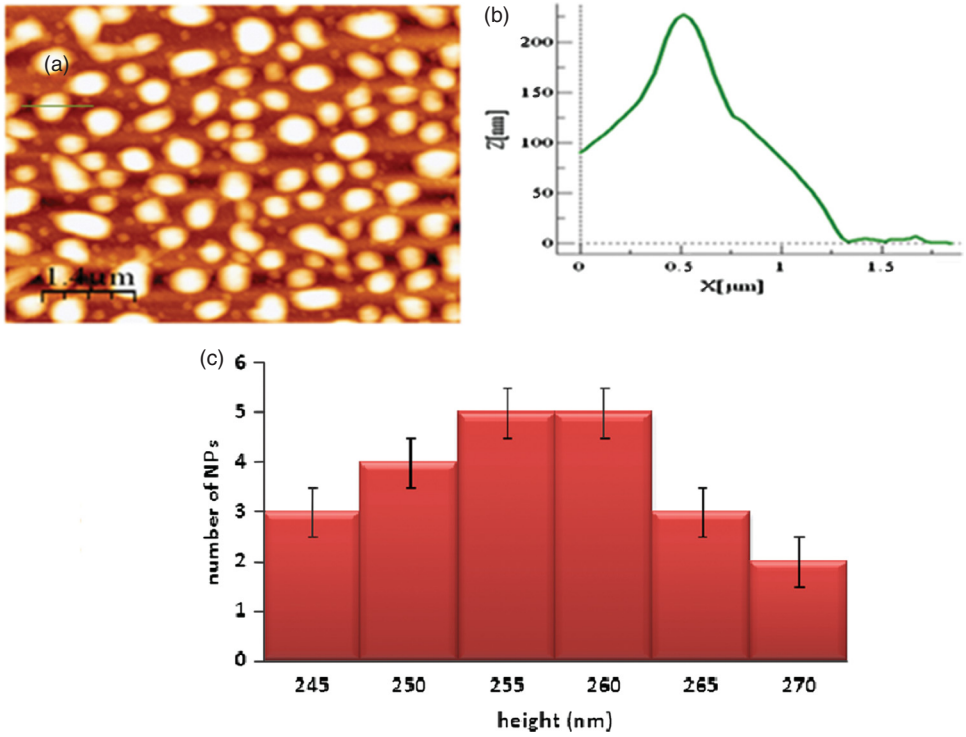

Fig. 6. (a) AFM images for NPs loaded 5-FU at different scanning size. (b) Cross-sectional height profile of single loaded NP, (c) Histogram shows the height distribution of drug loaded PLGA NPs.

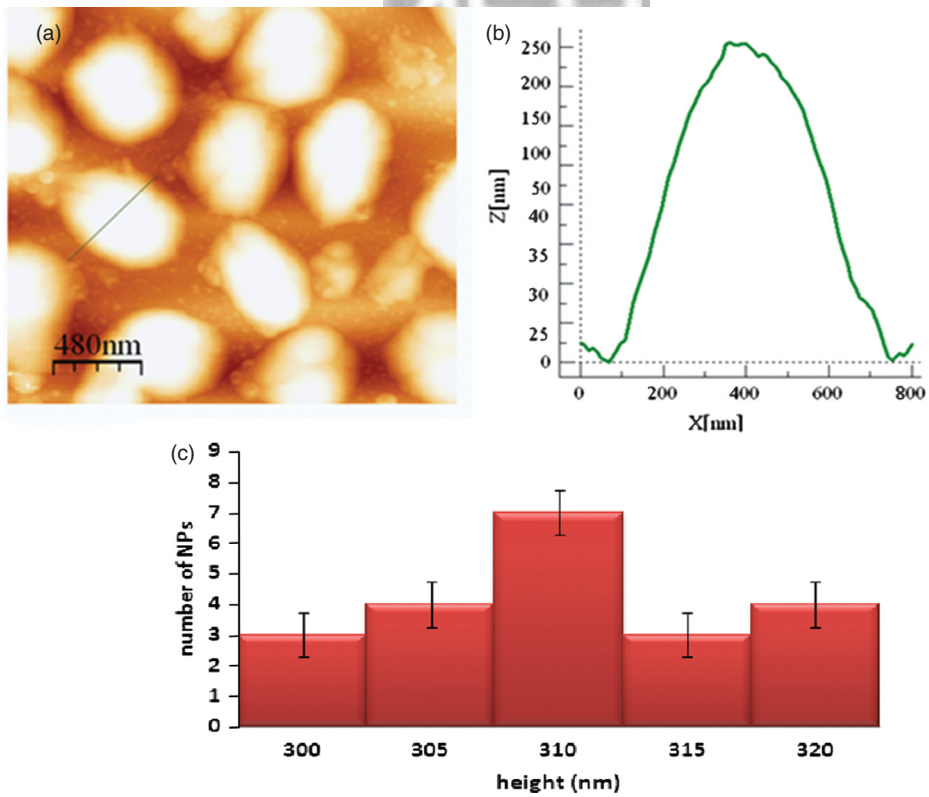

Fig. 7. (a) AFM image of gold/5-FU loaded nanoparticles. (b) Cross sectional height profile of single gold/loaded NP (c) Histogram shows the height distribution of gold/drug loaded PLGA NPs.

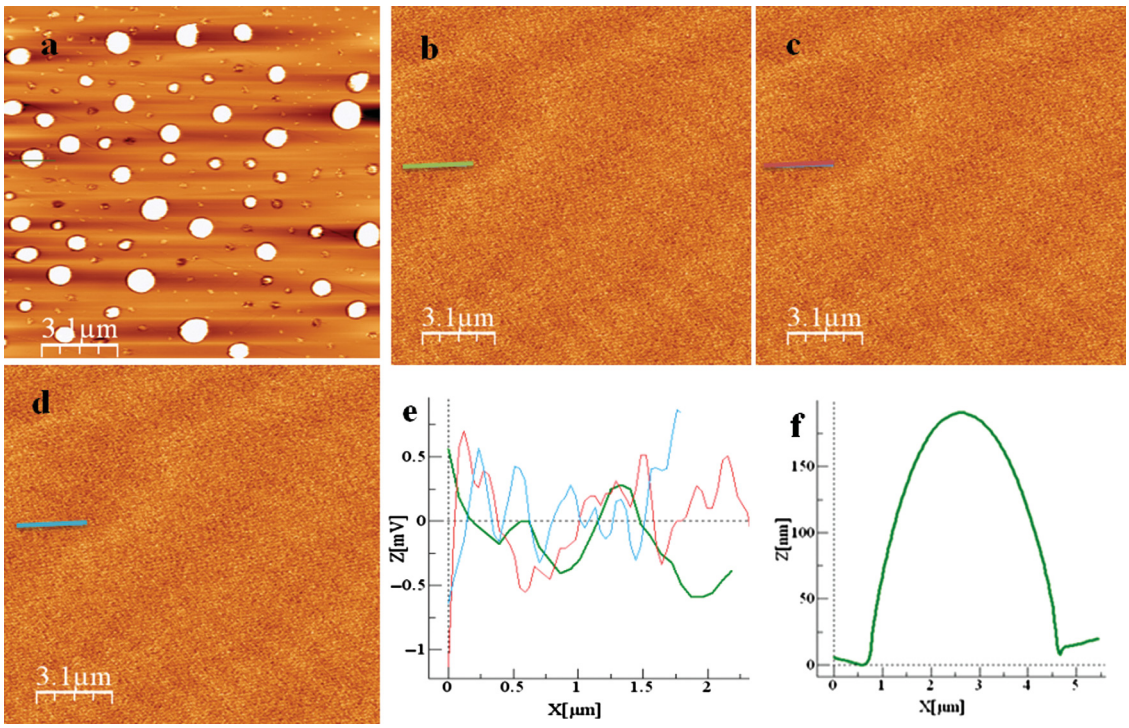

Fig. 8. (a) AFM image for empty nanoparticles. (b), (c) and (d) Shows EFM images for the same nanoparticles at +5 V, 0 V and −5 V respectively. (d) A line profile shows the magnitude of the signal on the PLGA nanoparticles. (f) Cross sectional height profile of single nanoparticle.

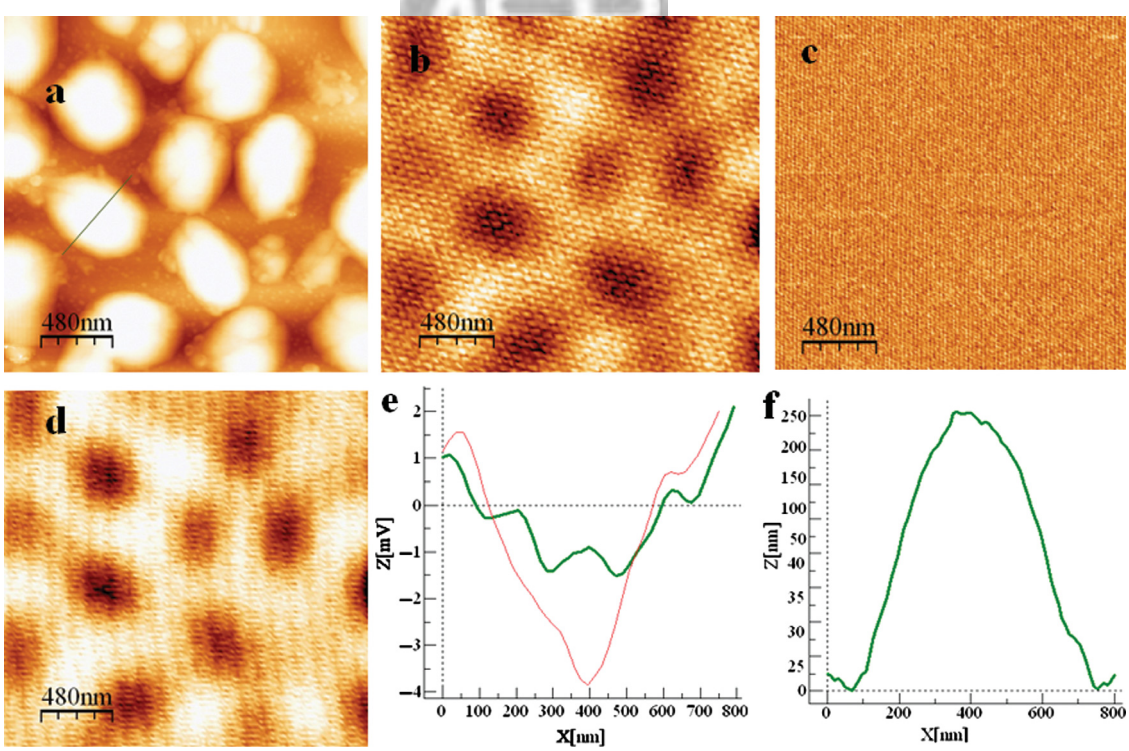

Fig. 9. (a) AFM image for 5-FU and gold nanoparticles loaded in PLGA nanoparticles. (b), (c) and (d) Shows EFM images for the same nanoparticles at +5 V, 0 V and −5 V respectively. (d) A line profile shows the magnitude of the signal on the loaded nanoparticles. (f) Cross sectional height profile of single nanoparticle.

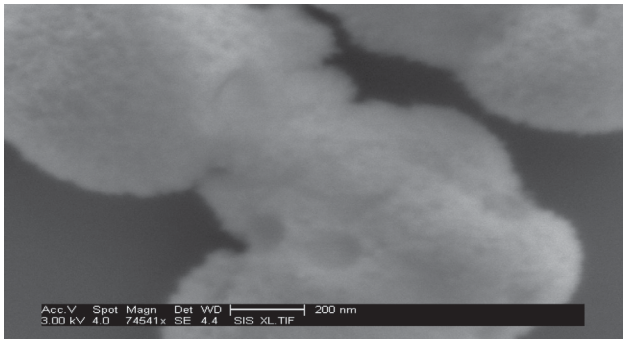

Fig. 10. A SEM image of two nanoparticles showing nanopores in the structure of the matrix.

loaded nanoparticles using two scanning amplifications. Figure 4(a) shows the detailed structure of two drug-loaded particles outlining the uniform shape of these drug delivery vehicles, while Figure 4(b) shows how these nanoparticles tend to cluster on the TEM grid.

Figure 5(a) shows a tapping mode AFM topography image of empty PLGA nanoparticles deposited on a mica substrate; with a cross sectional height profile (of a single NP) of 170 ± 54.130 nm as displayed in the profile shown in Figure 5(b). A histogram of the size distribution profile follows in Figure 5(c).

The morphology of the 5-FU loaded nanoparticles is shown in Figure 6. Upon loading, the size of nanoparticles increases by a factor of 30%, to reach approximately 250 ± 30.936 nm. A 3-D examination shows the relaxation of the nanoparticles on the mica surface in which the particles appear to be in the shape of a spheroid.

Drug-loaded gold nanoparticles topography images obtained using the AFM tapping mode are shown in Figure 7, in which the size of the particles has increased by about 64.7%. (From approximately 170 ± 54.130 nm for empty nanoparticles, to 280 ± 19.6 nm when gold was incorporated inside the PLGA nanovehicles.) As mentioned above, the shape of the nanoparticle can be described as that of a spheroid due of the relaxation of the PLGANPs on the mica surface.

Electrostatic force microscopy (EFM) is used to ensure the presence of the gold particles inside the loaded-PLGA drug carriers. EFM is one of the AFM modes for detecting the electrical properties of the object, and in our case neither the empty nanoparticles nor the drug loaded NPs are polarizable thus no electrostatic signal is emitted as shown in Figure 8. After loading the gold nanoparticles inside the carriers (via the roller-mixer), however, our newly synthesized 5-FU/PLGA/GNPs start to exhibit an electrostatic signal as evidenced by the black spots observed in EFM micrographs shown in the Figures 9(b and d).

The question still remains as to whether the gold nanoparticles are present on the surface of the drug loaded-PLGA nanovehicles or inside the PLGA matrix.

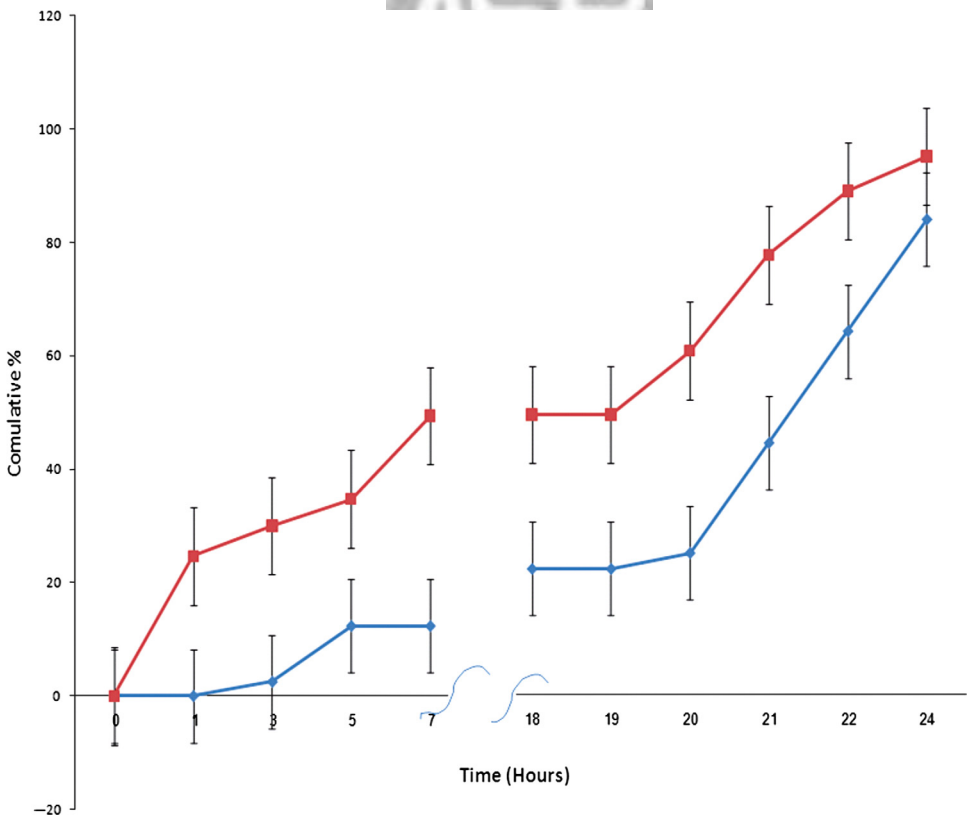

Fig. 11. Release profile of 5-FU from PLGA nanoparticles (blue line) and 5-FU from PLGA/GNPs (red line).

Figure 10(a) uses a high magnification of SEM to show the presence of ~100-nm nanopores in the 5-FU/ PLGA structure. We speculate that the 20-nm gold particles were able to diffuse, after 12 hours of mixing, into the PLGA matrix via these tiny pores without affecting the integrity of the drug delivery vehicle.

3.2. Size Analysis of Nanoparticles

After a 10-fold dilution with distilled water, the average size of nanoparticles, and their size distribution profiles are obtained using dynamic light scattering (DLS). The average size of the empty, drug-loaded, and gold/5-FU loaded nanoparticles are approximately 192.02 nm, 251.2 nm, and 316 nm, respectively. These results confirm the sizes measured using the AFM technique and reported earlier. We would like to elaborate more on how we compare the size of these nanoparticles using DLS and AFM. It is important to keep in mind that the total volume of the particles measured using both techniques is equal, however the shape is different due to the relaxation of the nanoparticles on the mica surface. Thus, the AFM shape of the PLGANPs shown in Figures 5–7 is assumed to be that of a spheroid with a volume $= 1/2a^2b$, where a is the Forward Width at Half Max (FWHM) and b is the AFM measured height as opposed to the DLS measurements which approximate the volume of these nanocarriers as a sphere ($V = 4/3\pi r^3$).

3.3. Determination of 5-FU Loading

Drug content, recovery and entrapment in the NPs are approximated using Eqs. (1–3) and UV spectrophotometer data. Approximately 26% of nanoparticles are recovered after drying. The percentage of total drug content is about 30%, and the percentage of drug entrapment reached 57%.

3.4. *In Vitro* Release

In vitro release of 5-FU from the PLGA nanoparticles is measured using the spectrophotometer UV absorbance data described previously. Figure 11 shows the cumulative percentage of 5-FU released from the two newly synthesized nanocarriers as a function of time. In the case of the 5-FU-loaded PLGA nanoparticles, the release shows a rapid initial phase, in which the drug located near the surface of the PLGA nanosystem diffuses out of the carrier at a considerably fast rate. But after this initial burst, the release plateaus for several hours as a result of the possible diffusion of some drug molecules back into the polymeric matrix. The release is resumed, afterwards, due to the erosion of the polymeric carrier. A similar release scenario unveiled with the drug-gold-loaded PLGA nanoparticles, but with one exception. The loaded GNPs appear to facilitate the release of the 5-FU molecules from the polymeric vehicle by aiding in the dissociation of the PLGA matrix. With both carriers, complete release appears to proceed within a period of 24 hours mainly due to the dissolution of the polymeric nanostructure.

4. CONCLUSION

The drug delivery system reported in this research consists of polymeric nanoparticles that are biocompatible and biodegradable, loaded with an antimetabolite chemotherapeutic agent and 20 nm-gold nanoparticles. The GNPs maybe utilized as photothermal agents inducing hyperthermia, thus enhancing the efficacy of regular drug loaded-PLGA nanoparticles. The nanoprecipitation method is chosen because of its simplicity and ability to form a homogeneous population of nanoparticles.

Morphological analysis for our newly designed nanosystem is performed using high resolution techniques including the tapping mode of AFM, and high resolution SEM and TEM. DLS indicates uniform nanoparticles with average diameters of 192.02 nm, 251.2 nm, and 316 nm corresponding to the empty NPs, drug loaded NPs and combined drug GPNs. Finally, *in vitro* release experiments prove that the gold nanoparticles aid in the dissociation of the polymeric NPs, which would facilitate the release of loaded drug.

The next step is to examine the feasibility of using this novel drug delivery system *in vitro*. To our knowledge, we are the first group to use EFM to study metallic nanoparticles incorporation inside polymer carriers. Additionally, while previous researchers have reported the deposition of gold on the surface of PLGA nanocarriers, here we show the presence of gold nanoparticles inside the PLGA matrix. We believe that the synergistic effect of the chemotherapy (induced by 5-Fluorouracil) coupled with the hyperthermia (induced by the gold nanoparticles) have the potential to increase the efficacy of these newly synthesized PLGA nanocarriers and may allow for decreasing the amount of the 5-FU administered to patient which in turn would reduce its cytotoxity and side effects.

References and Notes

1. M. Matsui, Y. Shimizu, Y. Kodera, E. Kondo, Y. Ikehara, and H. Nakanishi, *Cancer Sci.* 101, 1670 **(2010)**.
2. M. Hirai, H. Minematsu, Y. Hiramatsu, H. Kitagawa, T. Otani, S. Iwashita, T. Kudoh, L. Chen, Y. Li, M. Okada, D. S. Salomon, K. Igarashi, M. Chikuma, and M. Seno, *Int. J. Pharm.* 391, 274 **(2010)**.
3. P. Q. Zhao, H. J. Wang, M. Yu, S. Z. Cao, F. Zhang, J. Chang, and R. F. Niu, *Pharm. Res.* 27, 1914 **(2010)**.
4. G. A. Husseini, M. A. Diaz de la Rosa, T. Gabuji, Y. Zeng, D. A. Christensen, and W. G. Pitt, *J. Nanosci. Nanotechnol.* 7, 1 **(2007)**.
5. D. Stevenson-Abouelnasr, G. A. Husseini, and W. G. Pitt, *Colloids Surf. B-Biointerfaces* 55, 59 **(2007)**.
6. G. A. Husseini and W. G. Pitt, *J. Nanosci. Nanotechnol.* 8, 2205 **(2008)**.
7. W. G. Pitt, G. A. Husseini, B. L. Roeder, D. Dickinson, D. Warden, J. Hartley, and P. Jones, *J. Nanosci. Nanotechnol.* **(2010)**, In press.
8. G. A. Husseini, K. L. O'Neill, and W. G. Pitt, *Technol. Cancer Res. Treat.* 4, 707 **(2005)**.

RESEARCH ARTICLE

9. T.-F. Yang, C.-N. Chen, M.-C. Chen, C.-H. Lai, H.-F. Liang, and S.-W. Sung, *Biomaterials* 28, 725 **(2007)**.
10. Y. Bae, T. A. D. Ta, A. Zhao, and G. S. Kwon, *J. Controlled Release* 122, 324 **(2007)**.
11. J. You, X. Li, F. de Cui, Y. Z. Du, H. Yuan, and F. Q. Hu, *Nanotechnology* 19, 1 **(2008)**.
12. G. A. Husseini, W. G. Pitt, D. A. Christensen, and D. J. Dickinson, *J. Controlled Release* 138, 45 **(2009)**.
13. T. M. Goppert and R. H. Muller, *Int. J. Pharm.* 302, 172 **(2005)**.
14. C. Aschkenasy and J. Kost, *J. Controlled Release* 110, 58 **(2005)**.
15. S. Suttiruengwong, J. Rolker, I. Smirnova, W. Arlt, M. Seiler, L. Luderitz, Y. P. de Diego, and P. J. Jansens, *Pharm. Dev. Technol.* 11, 55 **(2006)**.
16. S. Jaspart, P. Bertholet, G. Piel, J. M. Dogne, L. Delattre, and B. Evrard, *Eur. J. Pharm. Biopharm.* 65, 47 **(2007)**.
17. S. Simovic and C. A. Prestidge, *Eur. J. Pharm. Biopharm.* 67, 39 **(2007)**.
18. S. Sashmal, S. Mukherjee, S. Ray, R. S. Thakur, L. K. Ghosh, and B. K. Gupta, *Pakistan J. Pharm. Sci.* 20, 157 **(2007)**.
19. G. Katsikogianni and K. Avgoustakis, *J. Nanosci. Nanotechnol.* 6, 2080 **(2006)**.
20. E. Leo, A. Scatturin, E. Vighi, and A. Dalpiaz, *J. Nanosci. Nanotechnol.* 6, 3070 **(2006)**.
21. F. H. Meng, G. H. M. Engbers, and J. Feijen, *J. Controlled Release* 101, 187 **(2005)**.
22. W. Jong and P. Borm, *Int. J. Nanomedicine* 3, 133 **(2008)**.
23. T. Govender, S. Stolnik, M. C. Garnett, L. Illum, and S. S. Davis, *J. Controlled Release* 57, 171 **(1999)**.
24. J. Yang, C. H. Lee, J. Park, S. Seo, E. K. Lim, Y. J. Song, J. S. Suh, H. G. Yoon, Y. M. Huh, and S. Haam, *J. Mater. Chem.* 17, 2695 **(2007)**.
25. H. Park, J. Yang, J. Lee, S. Haam, I. H. Choi, and K. H. Yoo, *ACS Nano* 3, 2919 **(2009)**.
26. H. Fessi, F. Puisieux, J. P. Devissaguet, N. Ammoury, and S. Benita, *Int. J. Pharm.* 55, R1 **(1989)**.

Received: 17 January 2011. Accepted: 20 January 2011.